South African Journal of Botany 168 (2024) 112–123

Contents lists available at ScienceDirect

South African Journal of Botany

journal homepage: www.elsevier.com/locate/sajb

The antimicrobial effectiveness of *Rosmarinus officinalis, Lavandula angustifolia*, and *Salvia officinalis* essential oils against *Klebsiella pneumoniae* and *Pseudomonas aeruginosa in vitro* and *in silico*

Fatima Mourabiti[a,b], Reda Derdak[a,c], Abdelaziz El Amrani[d], Ghizlane Momen[e], Mohammed Timinouni[f], Abdelaziz Soukri[a], Bouchra El Khalfi[a,*], Yassine Zouheir[b]

[a] *Laboratory of Physiopathology, Molecular Genetics & Biotechnology, Faculty of Sciences Ain Chock, Research Center of Health & Biotechnology, Hassan II University of Casablanca, 20100 Casablanca, Morocco*
[b] *Laboratory of Molecular Bacteriology, Pasteur Institute Casablanca, Casablanca, Morocco*
[c] *Department of Biology, Faculty of Sciences El Jadida, Chouaïb Doukkali University, B.P 20, El Jadida 24000, Morocco*
[d] *Laboratory of Molecular Synthesis, Extraction Valorization, Faculty of Sciences Ain Chock, Hassan II University of Casablanca, 20100 Casablanca, Morocco*
[e] *Laboratory of Mycobacteria, Pasteur Institute Casablanca, Casablanca, Morocco*
[f] *Laboratoire de Biotechnologie et bioinformatique, Ecole des Hautes Etudes de Biotechnologie et de santé (EHEB), Casablanca, Morocco*

ARTICLE INFO

Article History:
Received 17 October 2023
Accepted 6 March 2024
Available online xxx

Edited by: Dr I. Risenga

Keywords:
Essential oil
Resistant bacteria
Molecular docking
Drug-likeness
ADMET
In-silico
In-vitro
Antibacterial activity
Synergy
Combination

ABSTRACT

This study aimed to explore the phytochemical analyses and antibacterial potential of three essential oils (EOs) using both *in-vitro* and *in-silico* experiments for drug discovery. The Eos of *Rosmarinus officinalis, Lavandula angustifolia*, and *Salvia officinalis* were extracted by hydrodistillation, and GC–MS determined the chemical composition. The antibacterial activities of each EO were studied by the disc diffusion method. The minimum inhibitory concentration (MIC) and minimum bactericidal concentration (MBC) of these EOs were determined by micro-dilution. In addition, the EOs were combined with ineffective antibiotics (Aztreonam et al.) against clinical bacteria (*P. aeruginosa* and *K. pneumoniae)* to determine this association's effect. The *in-vitro* toxicological study was based on the MTT cytotoxicity assay. Finally, *in-silico* methods were employed to estimate their possible antibacterial mechanisms. Molecular docking was performed to calculate the predictive binding affinities of five major volatile components to three proteins key in the bacterial cycle using the AutoDock Vina program; prediction of drug-likeness properties and Toxicity prediction were carried out respectively by SwissADME and ProToxII online server. The results showed that the three EOs possessed antibacterial activity against ATCC and clinical *K. pneumoniae*. We note that *P. aeruginosa* was resistant to lavender and sage EOs. Surprisingly, adding EOs to antibiotics ineffective against resistant bacteria showed a significant synergistic antibacterial effect. Cytotoxicity assay of essential oils showed different values ranging from 0.22 to 0.43 μL/mL. Finally, the molecular docking study revealed that both compounds (1,8-Cineol, 1-Dodecene, Linalool, cis-Thujone, and Camphor) from the three EOs have a significant potential to inhibit the protein target involved in bacteria resistance. Furthermore, the SwissADME prediction results showed that all five components satisfy the rule of five and exhibit acceptable drug-like characteristics. findings suggest that the three EOs have interesting antibacterial activity. The *in-vitro* and *in-silico* studies gave a great potentiation and may constitute a promising option to control the emergence of MDR *P. aeruginosa* and *K. pneumoniae*.

1. Introduction

In recent years, antibiotic resistance has become one of the most worrisome health problems worldwide and is considered a global public health threat (WHO, 2021). Resistance and multi-drug resistance to antibiotics pose severe challenges for modern medicine. Novel antimicrobials are needed to continue treating antibiotic-resistant infections (Laxminarayan et al., 2013). The World Health Organization (WHO) has been concerned about the growing resistance of bacteria to antibiotics for several years. WHO has published the first list of the twelve antibiotic-resistant pathogens that pose the greatest threat to human health. Three categories exist depending on the urgency of the need for new antibiotics: critical, high, and medium priority (WHO, 2021). Among the most problematic multi-drug-resistant (MDR) organisms commonly encountered are *Klebsiella pneumoniae* and *Pseudomonas aeruginosa.* Infections caused by these bacteria are costly in terms of health care and continue to

* Corresponding author.
E-mail address: bouchra.elkhalfi@gmail.com (B. El Khalfi).

https://doi.org/10.1016/j.sajb.2024.03.015
0254-6299/

multiply over the years. In this context, the development of new antibacterial agents has become more interesting than ever and needs to be pursued (Jankauskaitė et al., 2016).

Traditional pharmacopeia has a rich source of molecules known for their antibacterial effect. The beneficial properties of the essential oils (EOs), including antibacterial properties, were discussed (E. et al. et al., 2020). EOs are aromatic, volatile liquids extracted from plant materials such as flowers, seeds, leaves, buds, herbs, bark, wood, fruits, and roots (Ayub et al., 2018). The *Lamiaceae* family is one of the most distinctive and significant flowering plants. Various parts of these plants are often aromatic, including Rosemary, Lavender, and Sage (Mseddi et al., 2020). *R.officinalis* belongs to the *Lamiaceae* family and is a precious medicinal plant; it contains various natural bioactive compounds with different pharmacological effects, especially antimicrobial potential (Lešnik et al., 2021). Throughout history, lavender products have been used as therapeutic agents for their antibacterial effects, and the antimicrobial activity of the essential oil of lavender against bacteria and fungi has long been established (Yang et al., 2020). Sage species are known for their many pharmacological activities and recognized antimicrobial effects (Conde-Hernández et al., 2021).

Therefore, the aim of this work, in particular, is to investigate the chemical composition of three essential oils obtained from rosemary, lavender, and sage. Additionally, evaluate the antibacterial activity of three EOs and determine the minimum inhibitory and bactericidal concentrations against susceptible and resistant bacteria. Then, study the effect of combining EOs with ineffective antibiotics against resistant bacteria. Herein, to reach this objective, molecular docking and drug-likeness properties of the major volatile compounds were also employed against target proteins associated with bactericidal/bacteriostatic effects such as DNA gyrase, Penicillin-binding-protein and quorum sensing LasR binding domain to identify better a possible mechanism of action correlated with the recorded antimicrobial activity of the potent essential oils.

2. Materials and methods

2.1. Plant material and hydrodistillation

Three aromatic plants growing in different regions of Morocco: *Rosmarinus officinalis* (RO) (Sutherland, 2008) was collected in Juin from Errachidia, *Lavandula angustifolia* (LA) (Govaerts, 2003) was obtained in April from Khemissat region, and *Salvia officinalis* (SO) (Govaerts, 2003) was collected from Meknes in May 2021. The study employed the dried leaves of these plants, and essential oils were extracted by hydrodistillation in a Clevenger apparatus for three hours. The chemical volatile composition of the essential oils was analyzed by gas chromatography-mass spectrometry (GC/MS).

2.2. Gas chromatography analysis

GC–MS units were performed using a Shimadzu GC/2010 Plus gas chromatograph equipped with a flame ionization detector (FID) and a BP-5 capillary column (30 m x0.25 mm i.d., film thickness 0.25um SGE Ltd), and interfaced with a Shimadzu Qp2010 Plus mass spectrometer (software version 2.50 SU1). The oven temperature was programmed as described for GC analysis: transfer line temperature, 300 °C; ion source temperature, 200 °C; carrier gas, helium, adjusted to a linear velocity of 36.5 cm.s^{-1}. Split ratio 1:40; ionization energy, 70 eV; scan range, 40 400 u; scan time, 1 s. Component identification was carried out by comparison of their retention indices relative to C9-C20 n alkanes on the BP-5 column (Adams., 2007), confirmed by comparison of recorded mass spectra with those of a computer library (Shimadzu corporation library and NIST05 database/ ChemStation data system) and from a home-made library, constructed based on the analyses of reference oils, laboratory-synthesized components and commercially available standards and other literature data (Essaqui et al., 2007).

2.3. Bacterial strains and growth

Microbial strains were used in the antibacterial activity assay, which included two ATCC strains, *Pseudomonas aeruginosa* ATCC 27,853 (*P. aeruginosa*) and *Klebsiella pneumonia* ATCC13883 *(K. pneumoniae),* which were purchased from American Type Culture Collection and two clinical strains (*P. aeruginosa* and *K. pneumoniae*) were isolated from urinary tract infections.

Conventional microbiological procedures were adopted for bacterial isolation. The identification of the clinical strains was confirmed by Gram stain. Then, each sample was streaked simultaneously onto different types of culture media, including Luria-Bretani, MacConkey agar, and Cetrimide agar plates, to isolate bacteria from urine samples.

2.4. Identification of bacteria

Biochemical tests were performed using the API 20E/NE system (bioMerieux, France) according to the manufacturer's directions to complete the diagnosis (Sawant et al., 2007). Bacteria strains are maintained as glycerol stocks in the Laboratory of Bacteriology, Pasteur Institute of Morocco in Casablanca. Glycerol stocks were streaked on nutritive agar to obtain fresh cultures to be used for all further studies.

2.5. Antibiotic susceptibility

The phenotypic susceptibility and resistance to antibiotics (ATBs) of *P. aeruginosa* and *K. pneumoniae* bacteria isolated from patients. We performed an antibiotic susceptibility assay following standards (CLSI, 2020). To determine the resistance profile of the two isolated bacteria, we began by inoculating the MH agar surface of each petri dish with a 0.5 McFarland bacterial suspension by swabbing. After 15 to 20 min drying time, we applied the ATB disks on the agar, Gentamicin (GEN 10ug), Nétilmicine (NET 30ug), Ticarcilline + acide clavulanique (TCC 10ug), Iimipenem (IPM 10ug), Tobramycine (TM 10ug), Amikacine (AN 30ug), Aztreonam (ATM 30ug), Ceftriaxone (CRO 30ug) Meropenem (MEM 10ug), Ciprofloxacin (CIP 5ug) and Ampicillin (AMP 10ug) on plates inoculated with clinical strains of *K. pneumoniae* and *P. aeruginosa*. The plates were then incubated at 37 °C for 18 to 24 h.

2.6. Antibacterial effect screening

2.6.1. Agar disc diffusion

The antibacterial activity of the three EOs was performed by an adapted agar diffusion technique (as recommended by CLSI, 2020), as previously described. With slight modifications (Chbel et al., 2022).

Before the sensitivity evaluation of the three EOs, each bacteria strain was cultured on nutrient broth (Luria Bertani) and incubated at 37 °C for 18 to 24 h. Then, from the fresh culture, a single colony was suspended in sterile distilled water adjusted to a turbidity of 0.5 McFarland (1×10^6 Colony Forming Units (CFU) / mL) using the Turbidimeter (Oxoid, UK).

After that, inoculation of the MHA agar using a soaked sterile cotton swab of inoculum of the strain to be tested, then applied on the surface of the agar plate until the plate has been swabbed in three directions across all the plates. Thus, the discs were applied gently to the surface of the agar plates. Subsequently, we placed in each petri dish a commercial antibiotic (IPM 10ug) disc for which the bacterium is susceptible which serves as a positive control, an empty sterile cellulose disc (6 mm in diameter) soaked in sterile distilled water as a negative control and small discs about 6 mm diameter size were

impregnated with 10 μL solution of the EOs then these saturated paper discs were inoculated at the center of each petri dish having bacterial lawn. Afterward, all Petri dishes were incubated at 37 °C for 18–24 h. Finally, the antibacterial activity was evaluated by measuring the diameters of the inhibitory regions observed around the EOs and denoting them as "mm." The experiments were repeated three times.

2.6.2. Microdilution assay

The broth microdilution assay was used to determine the minimal inhibition concentration (MIC), according to the Clinical and Laboratory Standards Institute (CLSI, 2020). All tests were performed in Mueller Hinton Broth (MHB, Oxoid, Basingstoke, UK). The bacterial strains were cultured overnight at 37 °C in MHA. The tested strains were suspended in MHB to give a final density of 10^6 cfu/mL.

50 μL of MHB was added to each 96-well micro-titer plate, and 100 μL of MHB was added to the 10th well for sterility control. MHB with 5 % DMSO was added to the ninth well for the growth control. Fifty microliters of solution of each Eos was added into the first well. A serial 2-fold dilution was performed by transferring 50 μL of the suspension to the subsequent wells up to the 10th well; bacterial inoculum of 0.5 McFarland will be diluted in the ratio of 1:100 and added into the 1st–10th wells to achieve the final concentration of 5×10^5 cfu/mL. The 11th well will be a sterility control, containing only the MHB. The 12th well was a growth control, containing only bacterial suspension.

2.6.3. Minimal bactericidal concentration (MBC) determination

To determine the MBC, wells that did not exhibit any growth in the MIC assay were cultured on freshly prepared MHA, and then they were incubated at 37 °C for 24 h. After incubation, the least concentration (highest dilution) inhibited colony formation on a solid medium was considered MBC (Khomarlou et al., 2018).

2.6.4. Effect of combination EO/ineffective antibiotic

For the two resistant bacteria (*P. aeruginosa* and *K. pneumoniae*), we studied the effect of combining each EO with some antibiotics to which these bacteria are resistant. The choice of these antibiotics for this test is based on the results obtained from the antibiogram carried out for the two clinical strains. Adding 10 μL of EO to the standard antibiotic disc using the disc diffusion method recommended by Shaaban et al. (2013). Then, inhibition zone diameters were measured. The experiments were performed in triplicate.

2.7. in-vitro *analyses cytotoxicity*

The cytotoxicity effect of EOs was determined in L929 fibroblast cell line of mouse using the 3-(4,5-dimethylthiazol-2-yl)−2,5-diphenyl tetrazolium bromide) (MTT) method as described by Gavanji et al. (2014) . Concentrations from the three EOs that reduce cells' vitality (IC_{50}) were calculated with the following equation using corrected absorbance:

Percentage cytotoxicity = (100 x (control - sample)).

All tests and analyses were run in triplicate, and mean values were recorded.

2.8. Molecular docking experiment

2.8.1. Protein preparation

In the present study, we have selected various bacterial target proteins such as penicillin-binding protein (PBP), DNA gyrase, and LasR domain binding protein. These proteins play an essential role in the life cycle of bacteria. Based on its role, we have selected these protein targets. The crystal structure was obtained from the RCSB PDB database (https://www.rcsb.org/) and downloaded -as a PDB file with the PDB ID; DNA Gyrase (PDB ID: 1KZN), Penicillin-binding Protein (PDB ID: 3UDI) and LasR (PDB ID: 2uv0). Its crystal structures for *in-silico* studies were used using Pymol and AutoDock Tools of the Vina program (Trott and Olson, 2009). The PDB files were energy minimized, the non-essential water molecules were removed, and polar hydrogen atoms to the receptors were merged. As well, the grid was specified. After that, the structure of the proteins was saved in PDBQT format for further analysis.

2.8.2. Ligand preparation

Five major chemical compounds determined in RO, LA, and SA (1,8-Cineol, Camphor, Linalool, 1-Dodecene, and cis-Thyjone) that can potentially be used as ligands were studied to detect their antibacterial activities against *K. pneumoniae* and *P. aeruginosa*. All chemical structures of ligands selected for the docking experiment were retrieved from the PubChem database (https://pubchem.ncbi.nlm.nih.gov/), their 3D structure was downloaded in an SDF format (structure data file), and then converted into PDB (Protein Data Bank) format using Pymol. AutoDock Tools are used to translate ligands into PDBQT format. They were prepared for molecular docking studies.

2.8.3. Molecular docking of major compounds in the three essential oils

Molecular docking of proteins of interest was conducted using Autodock Vina Version 1.5.7. All the PDBQT structures of ligands were docked in the binding sites of the receptors using the standard parameters of Autodock Vina (Trott and Olson, 2009). The docking scores were calculated as the predicted binding free energies (in kcal/mol). Biovia Discovery Studio Visualizer 2021 was used to identify H-bonds and non-bonding interactions between ligand-receptors and investigate the complex structures interacted with amino acids and docked poses on a 2D diagram.

2.8.4. In-silico *drug-likeness prediction for major compounds in the three essential oils*

Drug likeness activity, toxicity prediction, and ADMET screening of phytocompounds selected were conducted to see whether any natural compounds met the drug-likeness requirements. Lipinski's rule of five (Lipinski et al., 2001) was used to estimate drug-likeness characteristics. The rule predicts that there is likely to be poor absorption or permeation when a component possesses a number of hydrogen donors (should not be more than 5), the number of hydrogen acceptors (should not be more than 10), partition coefficient log P (should be less than 5) and molecular weight (mass should not be more than 500 Daltons), through the online tool SwissADME (http://www.swissadme.ch/). To examine all these, the 3D structure of the shortlisted hits selected was saved in canonical simplified molecular input line entry system (smile) format from PubChem database (https://pubchem.ncbi.nlm.nih.gov/) and uploaded on SwissADME. Furthermore, we evaluated the BOILED-Egg (Brain or Intestinal Estimated Permeation Method) to predict gastrointestinal absorption and brain penetration of the five compounds (Daina and Zoete, 2016). The boiled egg plot is a cartesian plan in the shape of an eclipse with three regions: white, grey, and yolk area. The white region for phytochemicals with a high probability of being absorbed by the gastrointestinal tract, the yolk area for molecules with a high probability of permeating the brain, and the grey zone for molecules with a low chance of being non-absorptive and non-penetrative. Blue dots represent molecules predicted to be P-Glycoprotein (PGP+) substrates and thus actively pumped from the brain into or into the gastrointestinal lumen. If no P-glycoprotein (PGP-) substrate is predicted, the corresponding point is red (Daina and Zoete, 2016).

To predict the toxicity class of the five ligands and their LD50 value tested, we used the Pro-Tox-II webserver (https://tox-new.charite.de/protox_II/index.php?site=compound_input).

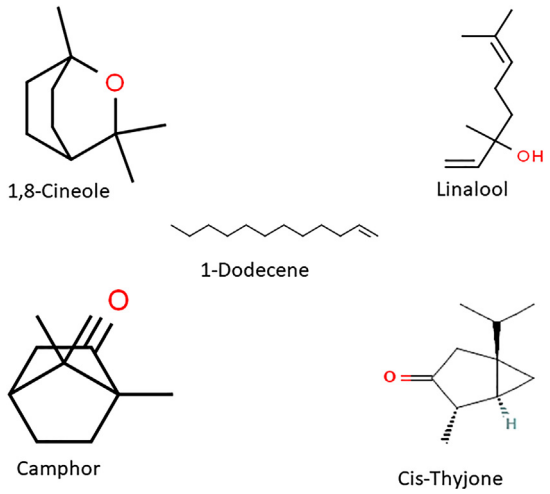

Fig. 1. Structures of major identified compounds of essential oils of RO, SA, and LA.

2.9. Statistical analysis

Mann-Whitney U test using SPSS 20.0 for Windows (SPSS et al.) was used to analyze the differences in inhibition zone diameters between groups. The data are given as means of three experiments ± one standard deviation.

3. Results

3.1. Phytochemical components of the essential oils

The chemical composition of *R. officinalis* "RO", *L. angustifolia* "LA", and *S. officinalis* "SA" essential oils was conducted by GC–MS technique. The results are presented in Table1, Table2 and Table3. This revealed the presence of 16 bioactive compounds representing 96.3 % of the total EO in RO, 19 in LA comprising 95.79 %, and 30 compounds representing 91.18 % in LA of the total composition of the EO. The main component in RO was 1,8-cineol (47.6 %) in RO. Two major volatile constituents identified include 1-Dodecene (32.65 %) followed by Linalool (29.51 %) in LA and cis-Thujone (24.98 %) followed by Camphor (22.28 %) in SA (Fig 1).

3.2. Antibiotic susceptibility

The antibiotic profile resistance of each strain was evaluated by the disc-diffusion method using several drugs, and the results are represented in Table 4. The results showed that *P. aeruginosa* is resistant to AMP, CIP, and MEM and sensible to GEN, TCC, ATM, TM, NET, CRO, and IPM, while *K. pneumoniae* is sensible to AMP, GEN, TCC, TM, NET, CIP, IPM and resistant to MEM and ATM.

3.3. Antibacterial Activity of the Studied Essential Oils

3.3.1. Disc Diffusion Method

This qualitative analysis revealed that all EOs studied exhibited considerable antibacterial activity against the four bacterial strains (both ATCC and resistant), showed important antibacterial effects (based on inhibition zone diameter = IZD) against *K. pneumoniae,* especially, RO EO was extremely influential on *K. pneumoniae* ATCC (IZD: 22 mm) but *P. aeruginosa* which was non-susceptible to EOs of LA and SO. The results of the inhibition zone diameters (IZD) obtained are summarized in Table 5.

3.3.2. Micro-dilution Method

Due to good inhibition of strains, a quantitative assay revealed two key parameters, namely, minimum inhibitory concentration (MIC) and minimum bactericide concentration (MBC) of each EO was determined by the microdilution technique, and these were utilized to show the efficiency of the used Eos. The results gave various MIC and MBC values, and the rosemary revealed the highest activities with MIC values ranging from 32,25 to 64.5 μL/mL and MBC with 125 μL/mL, followed by Lavender and then Sage. The results are shown in the Table 6.

3.4. Effect of association EO/ineffective antibiotics

In order to determine the type of interactions (synergy, additive effect, no effect, or antagonism) between EOs and ineffective antibiotics to improve their efficacy, a disc diffusion test is used. In total, the association of each effective EO with ceftriaxone (CRO) and aztreonam (ATM) to which *K. pneumoniae* was resistant showed higher ZIDs than those obtained with EO alone with significant differences ($p \leq 0.05$) (Table 7). Concerning resistant *P. aeruginosa*, only RO EO was tested in association with three ineffective antibiotics against this bacterium: ampicillin (AMP), ciprofloxacin (CIP), and meropenem (MEM). We found no significant difference between groups by comparing the results between ZIDs obtained by the RO alone and the RO/AMP and RO/MEM association ($p \geq 0.05$). However, the RO/CIP association demonstrated a significant difference ($p \leq 0.05$) between ZIDs (RO: 11 mm, RO/CIP: 16.5 mm) (Table 8).

3.5. Cytotoxic effects on the viability of L929 cells

The cytotoxic activity of the three Eos towards L929 cells was evaluated. The highest cytotoxicity was found with essential oil of Lavender, at a concentration of 0.22 μL/mL, inhibiting 50 % of cell growth. While at a concentration of 0.25μL/mL of rosemary, the IC50 value of *salvia oficinalis* reached 0.43 μL/mL.

3.6. Molecular docking experiment

In this study, five major constituents of EO extracted (1,8-cineol in RO, 1-Dodecene and Linalool in LA, Thujone-*cis* and Camphor in SA) and three proteins “key players in bacterial cell life and drug resistance process” (DNA Gyrase, Penicillin-binding protein, and LasR) were selected to conduct molecular docking. In docking results, the binding affinity (Docking Free energy) was presented in (Table 9).

The binding energy of the main volatile constituents with the target 1KZN was found in the following order: cis-thujone> linalool >1-dodecene>1,8-cineole>camphor. Furthermore, based on the binding affinity, phytocompounds tested could be arranged into an order of putative inhibition efficiencies for 8GPW cis-thujone>camphor>1,8-cineole>linalool>1-dodecene. And cis-thujone >1,8-cineole > camphor >1-dodecene > linalool for the target 2UV0.

Further, to get insights into the binding mechanism of the docked complexes, we performed 2D interaction analysis by Discovery Studio visualizer software, as shown in (Table 10 and Figs. 2,3 and 4). Results show that different types of intermolecular interactions formed the contact between the five major components and the three protein targets. For example, 1,8-cineole interacting with several residues via significant interactions, including alkyl with Ile90 and Ile78, and van-der-Waals with Glu50, Pro79, Asn46 and Met91, Camphor formed conventional hydrogen bonds with Asn46, van-der-waals with Pro79 and alkyl with Ile90 and Ile78, cis-thujone interacts Arg192 by alkyl interactions and with Ala 188, Leu205, Arg204, Leu191, Ile203, his217, Ser195, Aso214, his215 and Tyr218 by van-der-waals forces. 1-dodecene demonstrated six Alkyl bonds with Ile78, Ile90, Val43, Val167, Ala47, Val120 and six interactions van-der-waals with Thr165, Pro79, Glu50, Asn46, Asp73, Thr165 and

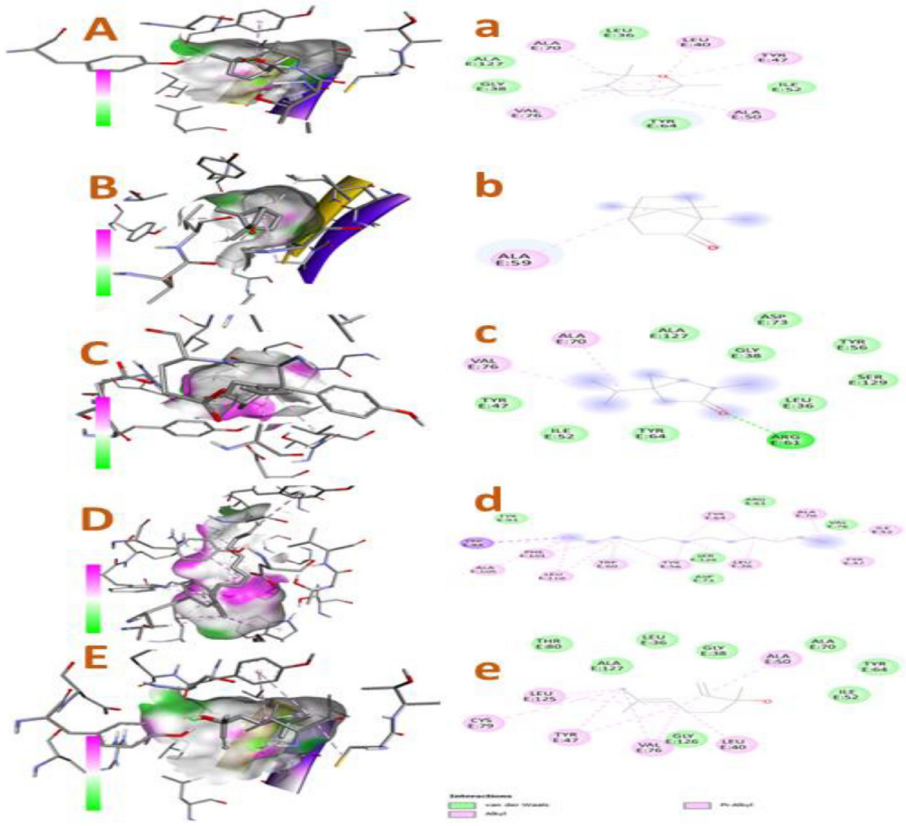

Fig. 2. 3D and 2D intermolecular interactions between the protein target LasR (2uv0) and the five major ligands. A, B, C, D, and E represent the 3D interactions between LasR and 1,8-cineole, camphor, cis-thujone, dodecane, and linalool, respectively. A, b, c, d, and e represent the 2D interactions between LasR and 1,8-cineole, camphor, cis-thujone, dodecane, and linalool, respectively.

Met91. Furthermore, one conventional hydrogen bond with Val43, three residues; Ile78, Ala47 and Val71 were implicated in alkyl interactions and nine residues formed van-der-waals interactions by Glu50, Asn46, Val44, Asp73, Ile90, Val120, Thr165, Val167 and Gln71. All these interactions formed between the five volatile components and the target 1KZN.

3.7. ADMET and drug-likness prediction

In the first step of *in-silico* prediction, the five ligands retrieved from PubChem were assessed using SwissADME software for Lipinski's Rule, Ghose rule, Muegge rule with drug-likeliness and physiochemical properties (Number of rotatable bonds, Number of Hydrogen bond donors, and Number of Hydrogen bond acceptors) as shown in Table 11. These revealed that the five compounds were accepted, passed Lipinski's Rule of five, and were soluble. Therefore, all of the ligands had a TPSA value less than 20 $Å^2$, except linalool, which had a value of 20.23$Å^2$.

Furthermore, the toxicity prediction and toxicity predicted class were evaluated by the ProToxII web application, which revealed that the range class of the selected compounds varied from 4 to 6 (Table 12).

3.8. Boiled-egg

In Fig 5. Boiled-egg images of the five examined ligands are given by SwissADME. The boiled egg image shows BBB (blood-brain barrier) permeation, HIA (human gastrointestinal absorption), PGP+, and PGP- properties. All the compounds 1,8-cineole, linalool, camphor, and cis-thujone are in the yellow region, except the 1-dodecene is in the grey region. As a result, all compounds are presented in red points.

4. Discussion

Phytochemical analysis of volatile oils from Rosemary, Lavender, and Sage using GC–MS had shown a richness in secondary metabolites depicted in (Tables 1, 2, and 3) belonging to various chemical classes, mainly monoterpenes, terpenes, and alkenes. The main components were 1,8-cineole (47.6 %) in RO, 1-dodecane (32.65 %), and linalool (29.51 %) in LA, cis-thyjone (32.98 %) and camphor (22.28 %). It has also been reported that 1,8-cineol (46.23 %) is the dominant compound in the EO of RO (from the middle Atlas region) (Hannour et al., 2018). While in another study from Rabat had linalool (44.67 %) and linalool acetate (42 %), the main compounds in LA (Slimani et al., 2022). However, a sample of SO from Taza contained as principal compounds detected were thujone (33.77 %), caryophyllene (12.28 %), humulene (12.19 %), camphor (11.52 %) (Al-Mijalli et al., 2022). These results have shown great genetic diversity in Morocco (Omurtag Özgen et al., 2022).

Many studies demonstrated that extracts of aromatic plants belonging to the family *Lamiaceae*, such as sage, lavender, and rosemary, have biological activity against bacteria (Mosafa et al., 2013). The antibacterial activity of EOs could be explained by their richness in monoterpenes compounds and terpenes, characterized by phenyl rings and hydroxyl groups in their chemical structures, which make them able to disrupt the outer membrane of Gram-negative bacteria, releasing lipopolysaccharides and increasing the permeability of the cytoplasmic membrane, resulting in ATP leakage. In addition, terpene compounds are also known to have antimicrobial activities (Miladi

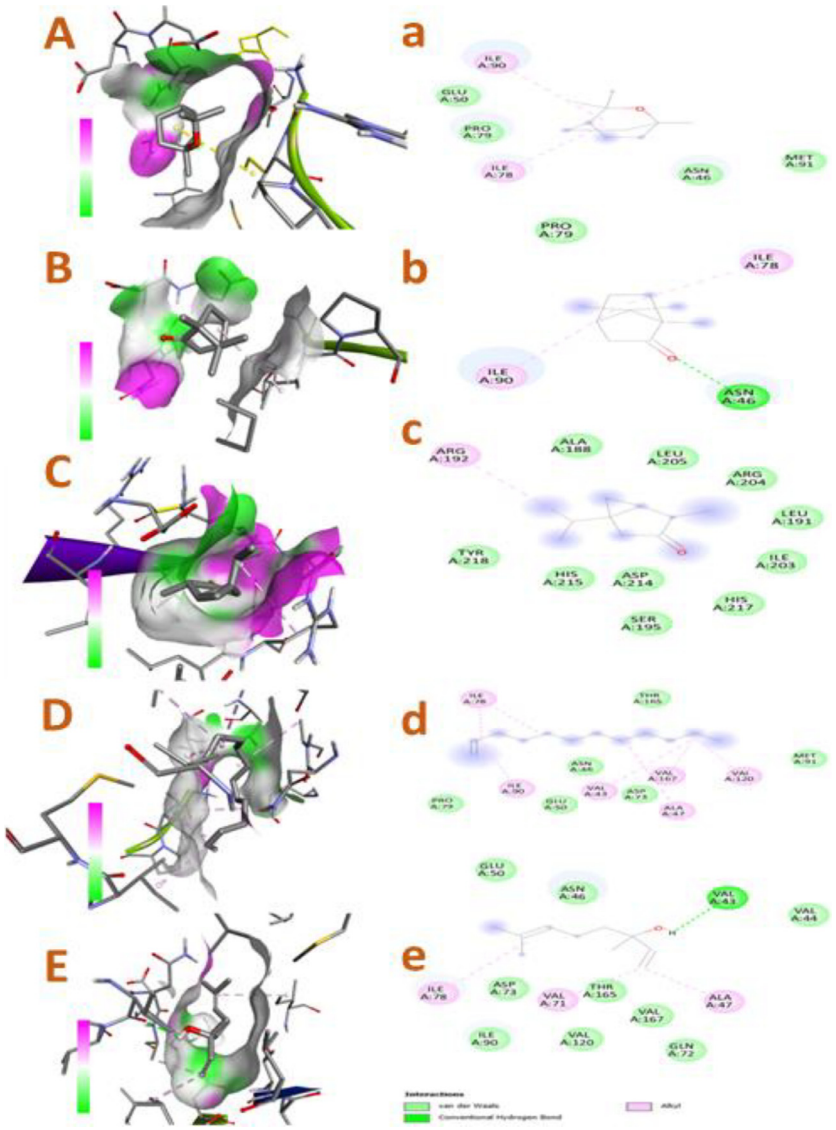

Fig. 3. 3D and 2D intermolecular interactions between the protein target DNA gyrase (1KZN) and the five major ligands. A, B, C, D, and E represent the 3D interactions between 1KZN and 1,8-cineole, camphor, cis-thujone, dodecane, and linalool, respectively. A, b, c, d, and e represent the 2D interactions between LasR and 1,8-cineole, camphor, cis-thujone, dodecane, and linalool, respectively.

et al., 2017). In this respect, it was essential to investigate the antibacterial potential of Rosemary, Lavender, and Sage.

In this work, we found that *RO* essential oil was the most effective, which demonstrated an antibacterial effect on all tested strains with IZDs ranging from 9 to 22.5 mm (table 4). According to (López et al., 2005), results showed that rosemary oil has an antibacterial effect on *P. aeruginosa* and *K. pneumoniae*. Another study conducted showed that RO EO has low inhibitory activity related to its richness in 1,8-cineole, camphor, and α-pinene, which are known to have weaker antimicrobial effects than phenolic and alcoholic compounds (Mulyaningsih et al., 2010).

LA and *SO* EOs did not act on *P. aeruginosa* but showed an antibacterial effect on *K. pneumoniae* strains (Tables 5 and 6). This is similar to another study conducted by Hossain et al. (2017), who tested several strains of *P. aeruginosa* and were all resistant to *LA* EO (Hossain et al., 2017). Another similar result was found in another study concerning the lack of effectiveness against the *P. aeruginosa* strain that is proven resistant, and this is explained by the fact that it is an opportunistic pathogen that often presents a resistance to antibacterial. This resistance could result from an external membrane that is mainly impermeable to phenolic compounds and the existence of efflux and inhibition mechanisms linked to porins that protect the bacteria against the action of Eos (Prabuseenivasan et al., 2006). However, in another study, the mechanism is more complex in *P. aeruginosa*, which may explain its resistance (Lister et al., 2009).

Several approaches have been developed to combat this growing challenge, including the search for natural antimicrobial agents with less toxicity and higher efficacy than those already in use. The use of EOs as plant-based products has been considered a very encouraging alternative to reduce the emergence of antimicrobial resistance due to their broad spectrum of antimicrobial activities and their exceptional chemical richness (Alaoui Jamali et al., 2017). For that, we carried out the antibiotic susceptibility test with the most used antibiotic against *P. aeruginosa* and *K. pneumoniae*. which showed (Table 4) that *P. aeruginosa* is resistant to AMP, CIP and MEM and sensible to GEN, TCC, ATM, TM, NET, CRO and IPM. At the same time, *K. pneumoniae* is sensible to AMP, GEN, TCC, TM, NET, CIP, and IPM and resistant to MEM and ATM. Then, we chose ineffective antibiotics in the combination assay with essential oils. The ability to potentiate the antibiotic activity by EOs has been investigated, aiming to increase its effectiveness against resistant bacteria.

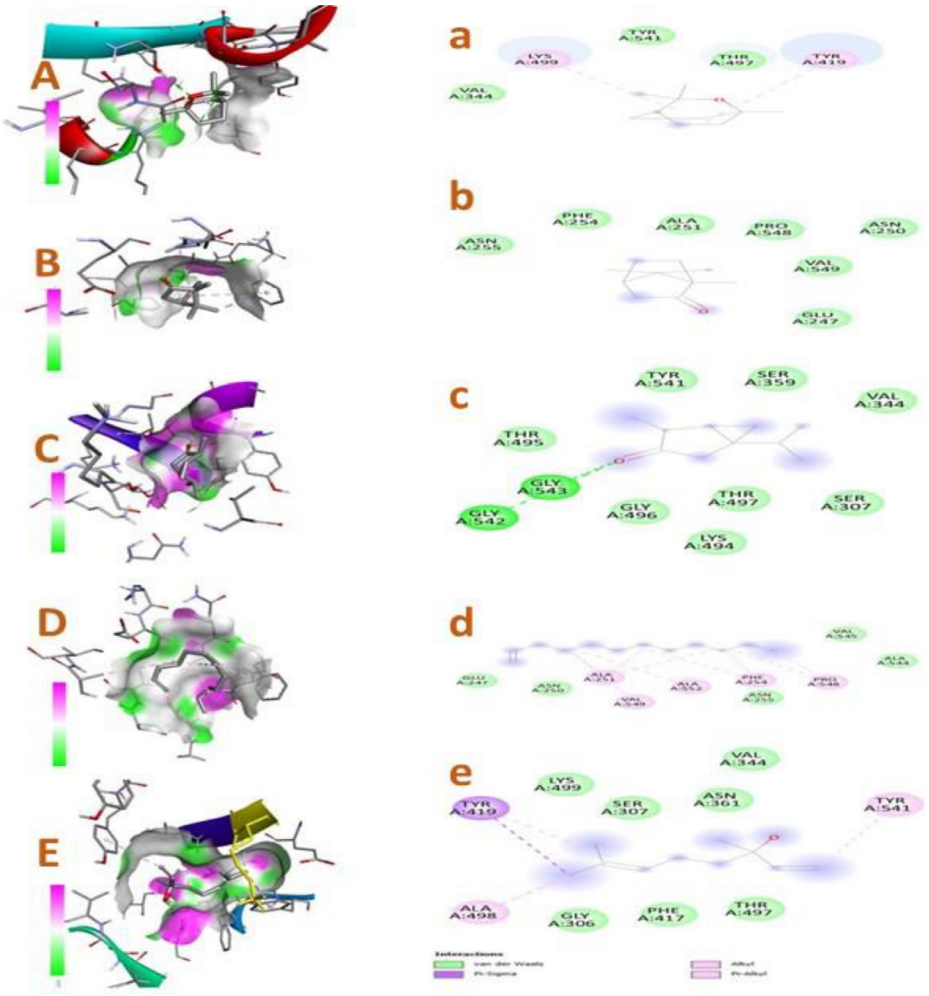

Fig. 4. 3D and 2D intermolecular interactions between the protein target PBP (8GPW) and the five major ligands. A, B, C, D, and E represent the 3D interactions between 8GPW and 1,8-cineole, camphor, cis-thujone, dodecane, and linalool, respectively. A, b, c, d, and e represent the 2D interactions between LasR and 1,8-cineole, camphor, cis-thujone, dodecane, and linalool, respectively.

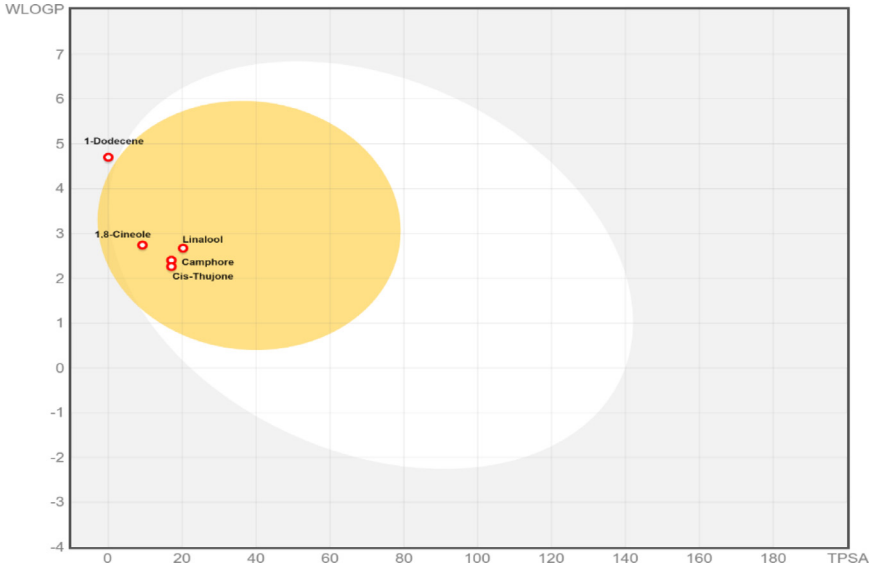

Fig. 5. Predictive model brain or intestinal estimated permeation method (BOILED-Egg plot).

Table 1
Chemical composition of essential oil of *R. officinalis*.

N°	Name	% Area	RT	Chemical formula
1	α-Pinene	10,3	05.85	C10H16
2	Camphene	3,7	06.26	C10H16
3	ß-Pinene	3,8	07.04	C10H16
4	Myrcene	1,2	07.43	C10H16
5	Limonene	2,2	08.69	C10H16
6	**1,8-Cineole**	47,6	08.76	C10H18O
7	*P*-Cymene	1,6	08.53	C10H14
8	Camphre	10,4	13.28	C10H16O
9	Linalool	0,8	11.32	C10H18O
10	Bornyl Acetate	1,1	19.49	C12H20O2
11	Terpinene 4-Ol	0,9	14.66	C10H18O
12	ß-Caryophyllene	0,9	25.36	C15H24
13	α-Humulene	0,6	26.82	C15H24
14	α-Terpinéol	3,5	15.21	C10H18
15	Borneol	7,6	14.29	C10H18O
	Verbenone	Tr	15.97	C10H14O
Total		96,3		

Tr: traces.

Table 2
Chemical composition of essential oil L. *angustifolia*.

N°	Name	% Area	RT	Chemical formula
1	3-*Octanone*	0,47	07.19	C5H11C(O)C2H5
2	ß-Myrcene	1,45	07.43	C10H16
3	Hexyl Acetate	0,32	08.05	C8H16O2
4	Limonene	0,84	08.69	C10H16
5	Eucalyptol	1,1	08.76	C10H18O
6	cis-ß-Ocimene	4,67	08.96	C10H16
7	trans-ß-Ocimene	3,74	09.42	C10H16
8	**Linalool**	29,51	11.32	$C_{10}H_{18}O$
9	*allo Ocimene*	0,3	11.32	C10H16
10	Borneol	0,57	14.29	C10H18O
11	4-Terpineol	4,21	14.66	$C_{10}H_{18}O$
12	α-Terpineol	2,33	15.21	$C_{10}H_{18}O$
13	**1-Dodecene**	32,65	15.25	C12H24
14	Lavandulyl Acetate	3,47	19.70	$C_{12}H_{20}O_2$
15	1-Tetradecene	2,36	24.10	C14H28
16	Caryophyllene (Z)	4,09	24.95	C15H24
17	α-Santalene	0,42	25.31	C15H24
18	1-Hexadecene	2,06	32.44	C16H32
19	1-Octadecene	1,23	40.02	C18H36
Total		95,79		

Tr: traces.

Interestingly, we found that the association of the RO EO with CRO and ATM separately produced a synergistic effect against resistant *K. pneumonia (*Table 7*)*. A similar effect was verified when the RO EO was tested in association with CIP against resistant *P. aeruginosa* (Table 8). Several EOs and volatile compounds have been reported to increase the susceptibility of *K. pneumoniae* reference strains to conventional antibiotics. One study reported that the RO/CIP combination against *K. pneumoniae* displayed the most favorable synergistic pattern (Van Vuuren et al., 2009). One study investigating *Thymus maroccanus* and *Thymus broussonetii* EOs reported synergistic effects in combination with conventional antibiotics (ciprofloxacin, gentamicin, and pristinamycin) against *K. pneumoniae.* The production of this synergy is due to specific mechanisms of antimicrobial interaction, including inhibition of protective enzymes, combination of membrane-active agents, sequential inhibition of common biochemical

Table 3
Chemical composition of essential oils of *S. officinalis*.

N°	Name	% Area	RT	Chemical formula
1	Tricyclene	0,11	05.53	C10H16
2	α-Thujene	0,23	05.62	C10H16
3	α-Pinene	4,68	05.85	C10H16
4	Camphene	4,01	06.26	C10H16
5	Sabinene	0,14	06.91	C10H16
6	ß-Pinene	2,05	07.04	C10H16
7	ß-Myrcene	0,46	07.43	C10H16
8	P-Cymene	1,81	08.53	C10H14
9	Limonene	2,04	08.69	C10H16
10	Eucalyptol	10,6	08.76	C10H18O
11	Gamma-Terpinene	0,18	09.78	C10H16
12	Cis-Sabinene Hydrate	0,07	10.20	C10H18O
13	Terpinolene	0,06	10.98	C10H16
14	Linaloolcis-	0,19	11.32	C10H18O
15	**Thujone**trans-	24,98	11.56	C10H16O
16	Thujone-Trans-	7,08	12.00	C10H16O
17	Isothujol trans-	0,13	12.94	C10H16O
18	Sabinol	0,06	13.10	C10H16O
19	**Camphor**	22,28	13.28	C10H16O
20	4-Terpineol	0,38	12.77	C10H18O
21	α-Terpineol	0,16	15.21	C10H18O
22	1-Dodecene	0,4	15.25	C12H24
23	Bornyl Acetate	1,08	19.49	C12H20O2
24	Thymol	0,11	19.71	C10H14O
25	1-Tetradecene	0,62	24.10	C14H28
26	Caryophyllene (Z)	3,6	24.95	C15H24
27	α-Caryophyllene	2,65	25.36	C15H24
28	1-Octadecene	0,5	40.02	C18H36
29	1-Eicosene	0,36	46.92	C20H40
30	Sclareol	0,16	54.21	C20H36O2
Total		91,18		

Tr: traces.

pathways, and the use of membranotropic agents to enhance the diffusion of other antimicrobials (Fadli et al., 2012). Strong synergistic effects have been reported for the combinations between basil (*Ocimum basilicum*) EO and imipenem/ciprofloxacin against *the P. aeruginosa* reference strain and the clinical isolate (Silva et al., 2016). A recent study showed that the EO / antibiotic combination was effective against both resistant strains and biofilm formation of *P. aeruginosa*. The synergistic effect of EO with antibiotics was mainly due to the presence of rosmarinic, gallic, and benzoic acids, which decrease bacterial constituents (proteins, nucleic acids, and inorganic ions) by improving the permeability of the bacterial cytoplasmic membrane. Another interesting mechanism of gallic acid inhibits the supercoiling activity of bacterial gyrase by binding to the ATP binding site of gyrase B (W. W. Mohamed et al., 2020). Rosemary EO contains 1, 8-cineole, which damaged the shape and cell size of bacteria; the nucleus cytoplasm was reduced or agglomerated on the side, which can explain the antibacterial effect of this EO (Li et al., 2014).

LA EO had a remarkable antimicrobial effect on *K. pneumoniae* strains (Table 5,6). In comparison, the association of LA and the two ineffective antibiotics, ceftriaxone and aztreonam, against *K. pneumoniae* had potentiated its effect (Table 7). Another study conducted by Yang et al. (2020) detected the presence of a synergistic antibacterial effect against carbapenemase-producing *K. pneumoniae* when *LA* EO was associated with conventional meropenem; it was the result of oxidative stress induced by *LA* EO, which modifies the bacterial

Table 4
Profile of resistance of the studied strains to antibiotics.

	AMP	GEN	TCC	ATM	TM	NET	CIP	CRO	IPM	MEM
K. pneumoniae	+	+	+	–	+	+	+	–	+	–
P. aeruginosa	–	+	+	+	+	+	–	+	+	–

+: Sensibility, -: Resistance.

Table 5
Antibacterial activity of essential oils against bacterial strains by disc diffusion method.

Essential oil	Bacteria	Diameter of inhibition (mm)
Rosmarinus officinalis	*P. aeruginosa ATCC*	9.3 ± 0.7
	K. pneumonaie ATCC	22.53±1.06
	P. aeruginosa Clinical	12.53±0.35
	K. pneumonaie Clinical	11.3 ± 0.7
Lavandula angustifolia	*P. aeruginosa ATCC*	–
	K. pneumonaie ATCC	10.53±0.3
	P. aeruginosa Clinical	–
	K. pneumonaie Clinical	13.3 ± 0.7
Salvia officinalis	*P. aeruginosa ATCC*	–
	K. pneumonaie ATCC	9.3 ± 0.7
	P. aeruginosa Clinical	–
	K. pneumonaie Clinical	13.3 ± 1.06

Table 6
Minimum inhibitory concentration (MIC; μl /mL) and minimum bactericidal concentration (MBC; μl /mL) of essential oils against bacterial strains.

	Rosmarinus officinalis MIC MBC	*Lavandula angustifolia* MIC MBC	*Salvia officinalis* MIC MBC
P. aeruginosa ATCC	32.25 125	- -	- -
K. pneumonaie ATCC	64.5 125	125 125	125 250
P. aeruginosa Clinical	32.25 125	- -	- -
K. pneumonaie Clinical	64.5 125	125 125	250 250

Table 7
Effect of association between EOs and antibiotics for resistant *K. pneumonia*.

	EOs and CRO						EOs and ATM					
	RO	RO/CRO	SO	SO/CRO	LA	LA/CRO	RO	RO/ATM	SO	SO/ATM	LA	LA/ATM
ZIDs (mm)	12.5	17.5	13	17	13	21	12.5	15.5	13	15.5	13	17.5
***p* value**	$p \leq 0.05$		$p \leq 0.05$		$p \leq 0.05$		$p \leq 0.05$		$p = 0.1$		$p \leq 0.05$	

RO: R. officinalis; LA: L. angustifolia; SO: S. officinalis; CRO: ceftriaxone; ATM: aztreonam; IZD : inhibition zones diameter.

membrane permeability of *K. pneumonia.* The antimicrobial activity of EOs is a result of the antibacterial properties of major and minor chemical components, such as linalool and linalyl acetate, which are believed to be responsible for the antibacterial and antifungal properties of EOs (Yang et al., 2020).

EO of *SO* was effective against *K. pneumoniae* strains, whereas *P. aeruginosa* was resistant (Tables 5 and 6). At the same time, the association of SO EO had potentiated its effect against *K. pneumoniae* (Table 7). It was reported that the most prevalent synergistic interaction was noted when the EO of *S. officinalis* was combined with ceftriaxone and ciprofloxacin. Interestingly, the same combination of this EO and gentamicin exhibited a synergistic effect on other MRSA strains. The antimicrobial power is generally correlated with the chemical composition of the oil. The antimicrobial activity of *S. officinalis* could be attributed to components like α-thujone, 1,8-cineole, and camphor (Conde-Hernández et al., 2021). In this study, cis-thujone and camphor are the significant components of the essential oil SO.

The increase in EO concentration showed a significant cytotoxic effect on the adherent cells. The IC_{50} for L. *angustifolia, R. officinalis,* and *S. officinalis* were 0.22, 0.25 and 0.43 μL/mL respectively. In concordance with our findings, the EO of L. *angustifolia* described displaying cytotoxic effects on the human tumor cell line (HeLa cells) and peripheral blood cells with the IC_{50} of 26 and 21 μg/ml, respectively (Ghadri et al., 2010). Regarding the cytotoxic activity of *RO* EO, it was reported that it possessed potent inhibition of cell proliferation with IC_{50} = 3.06–7.38 μg/mL) (Gezici et al., 2017). Nevertheless, for other cell lines (SK-OV-3, HO-8910, Bel-7402), *RO* EO was found to be relatively non-toxic (IC_{50} ≥250 μg/mL) (Wang et al., 2012). Finally, *SO* EO was described as having less cytotoxicity in cancer cell lines with IC_{50} values greater than 260 μg/mL (El Hadri et al., 2010).

Molecular docking is a computational modeling tool to predict a small molecule's preferred conformation or orientation (ligand) when bound to a target macromolecule (receptor), such as a protein. The importance of molecular docking lies in its capacity to provide valuable insights into the molecular interactions between ligands and receptors (Chen et al., 2021). Molecular docking was performed employing AutoDock vina to understand better the molecular basis of the antibacterial potential provided by the five main volatile compounds of rosemary, lavender, and sage essential oils. Antibiotics target bacterial metabolism, limiting their growth by inactivating vital proteins involved in different critical bacterial processes to survive, such as DNA gyrase (PDB ID; 1KZN), LasR binding domain, and Penicillin-binding protein. DNA gyrase controls the topology of DNA during transcription and replication; since it is essential for bacterial survival, it is an important target for antimicrobial agents (Aliye et al., 2021). Penicillin-binding-protein "PBP" (PDB ID; 8GPW), which plays a key role in peptide cross-linking during peptidoglycan cell wall biosynthesis and its inhibition leading to bacterial cell lysis and death (Varela et al., 2021). The emergence of the quorum-sensing autoinducer LasR-binding domain (PDB ID; 2uv0) as a critical regulator of *P.*

Table 8
Effect of association between *R. Officinalis* EO and antibiotics for resistant *P. aeruginosa*.

	RO	RO/AMP	RO/CIP	RO/MEM
ZIDs (mm)	11	11	16.5	12.5
***p* values**		$p \geq 0.05$	$p \leq 0.05$	$p \geq 0.05$

RO: R. officinalis; AMP: ampicillin; CIP: ciprofloxacin; MEM: meropenem; IZD: inhibition zones diameter.

Table 9
Binding free energy values were calculated through molecular docking for the major volatile components of *R. officinalis,* L. *angustifolia, and S. officinalis* and the bacterial targets as receptors.

Ligand	Binding Free Energy(kcal/mol)		
	1KZN*	8GPW	2UV0
1,8-Cineole	−4.4	−4.8	−6.9
Camphor	−4.3	−4.9	−6.7
cis-Thujone	−5.6	−5.3	−7.0
1-Dodecene	−4.5	−4.3	−6.5
Linalool	−5.4	−4.7	−6.2

*Protein PDB ID; 1KZN: DNA Gyrase, 8GPW: Penicillin-binding protein and 2uv0: LasR.

Table 10
List the interacting amino acid residues involved in the ligand–protein interaction of the major compounds against three different targets.

	1KZN		8GPW		2UV0	
	Interacting Amino Acid	Type of Intermolecular Bond	Interacting Amino Acid	Type of Intermolecular Bond	Interacting Amino Acid	Type of Intermolecular Bond
1,8-Cineole	Ile90 Glu50 Pro79 Ile78 Asn46 Met91	Pi-Alkyl V-d-W** V-d-W Pi-Alkyl V-d-W V-d-W	Tyr419 Lys499 Thr497 Tyr541 Val344	Alkyl Pi-Alkyl V-d-W V-d-W V-d-W	Leu36 Ile52 Tyr64 Gly38 Ala127 Leu40 Tyr47 Ala50 Val76 Ala70	V-d-W V-d-W V-d-W V-d-W V-d-W Pi-Alkyl Pi- Alkyl
Camphor	Ile90 Pro79 Ile78 Asn46	Pi-Alkyl V-d-W Pi-Alkyl Hydrogen Bond	Ala251 Asn255 Phe254 Pro548 Asn250 Val549 Glu247	V-d-W V-d-W V-d-W V-d-W V-d-W V-d-W	Ala59	Alkyl
Cis-Thujone	Ala188 Leu205 Arg204 Leu191 Ile203 His217 Ser195 Asp214 His215 Tyr218 Arg192	V-d-W V-d-W V-d-W V-d-W V-d-W V-d-W V-d-W V-d-W V-d-W Pi-Alkyl	Tyr541 Ser359 Val344 Ser307 Thr497 Lys494 Gly496 Thr495 Gly543 Gly542	V-d-W V-d-W V-d-W V-d-W V-d-W V-d-W V-d-W Hydrogen Bond Hydrogen Bond	Ala127 Gly38 Asp73 Tyr56 Ser129 Leu36 Tyr64 Ile52 Tyr47 Ala70 Val76 Arg61	V-d-W V-d-W V-d-W V-d-W V-d-W V-d-W V-d-W V-d-W Alkyl Hydrogen Bond
1-Dodecene	Thr165 Met91 Asp73 Asn46 Glu50 Pro79 Val120 Val47 Val43 Ala47 Ile90 Ile78	V-d-W V-d-W V-d-W V-d-W V-d-W V-d-W Alkyl	Glu247 Asn250 Asn255 Val545 Ala544 Ala251 Val549 Ala552 Phe254 Pro548	V-d-W V-d-W V-d-W V-d-W V-d-W Alkyl Pi-Alkyl Pi-Alkyl	Tyr93 Arg61 Val76 Ser129 Asp73 Tyr64 Ala70 Ile52 Tyr47 Leu36 Tyr56 Leu110 Ala105 Trp60 Phe101 Trp88	V-d-W V-d-W V-d-W V-d-W V-d-W Alkyl Pi-Alkyl Pi-Alkyl Pi-Sigma
Linalool	Val71 Ala47 Ile78 Thr165 Asp73 Asn46 Glu50 Pro79 Val167 Val120 Ile90 Val44 Val43	Alkyl V-d-W V-d-W V-d-W V-d-W V-d-W V-d-W V-d-W V-d-W Hydrogen Bond	Lys499 Ser307 Asn361 Val344 Thr497 Phe417 Gly306 Tyr541 Ala498 Tyr419	V-d-W V-d-W V-d-W V-d-W V-d-W V-d-W V-d-W Pi-Alkyl Pi-Sigma	Thr80 Ala127 Leu36 Gly38 Ala70 Tyr64 Ile52 Gly126 Ala50 Leu40 Val76 Tyr47 Leu125 Cys79	V-d-W V-d-W V-d-W V-d-W V-d-W V-d-W V-d-W V-d-W Alkyl Pi-Alkyl Pi-Alkyl

*Protein PDB ID; 1KZN: DNA Gyrase, 8GPW: Penicillin-binding protein and 2uv0: LasR. **; V-d-W: Van der waals Forces.

Table 11
Physiochemical proprieties and drug-likeness prediction of phytoconstituents by drug-likeness rules evaluation using SwissADME.

Ligand	MW (g/mol)	logP	H-bond acceptors	H-bond donors	Lipinski Rule	Ghose filter	Muegge rule	TPSA (Å^2)	Solubility
1,8—Cineole	154.25	2.74	1	0	Yes	No	Yes	9.23	Soluble
Camphor	152.23	2.4	1	0	Yes	No	No	17.07	Soluble
Cis-Thujone	152.23	2.26	1	0	Yes	no	No	17.07	Soluble
1-Dodecene	168.32	4.7	0	0	Yes	yes	No	0.00	Moderately
Linalool	154.25	2.67	1	1	Yes	no	no	20.23	Soluble

aeruginosa pathogenesis makes its inhibition an interesting drug target (Rajalakshmanan et al., 2021).

The results of docking (Table 9) the five phytocompounds showed that Cis-Thujone had the low binding free energy score, which revealed that Cis-Thujone had the best affinity to each protein; 1kzn, 8GPW, and to 2UVO followed by linalool (−5.4 kcal/mol) against 1KZN, camphor (−4.9) against 8GPW and 1,8-cineole (−6.9) against 2UV0. Furthermore, we elucidate molecular interactions (Figs. 2, 3, and 4, table 10) between ligand-receptor by Discovery Studio. Which revealed that all the five components formed different types of interactions with residues of proteins. For example, cis-thujone bound to 1KZN by binding its residues; Ala188, Leu205, Arg204, Leu191 Ile203, His217, Ser195, Asp214, His215 and Tyr218 by van-der-walls and stabilized by Pi-alkyl interactions with Arg192. Moreover, forming two conventional hydrogen bonds with Gly543 and Gly542, and van-der-walls forces are established to bind the 8GPW Tyr541, Ser359, Val344, Ser307, Thr497, Lys494, Gly496, and Thr495, and it formed nine van-der-walls interactions with Ala127, Gly38, Asp73, Tyr56, Ser129, Leu36, Tyr64, Ile52 and Tyr47 however two Alkyl interactions were involved in stabilizing the complex cis-thujone with 2UV0 and one hydrogen bound with Arg61.

To propose some potential lead therapeutic components having acceptable drug-like properties, known as the five rules of Lipinski, drug candidate ligands are required to follow these rules, or the number of violations must be less than 4. Firstly, we used the online server SwissADME, which revealed that all the Five top compounds of essential oils from rosemary, lavender, and sage satisfy the rule of 5. Other rules are evaluated (Ghose and Muegge); just the 1,8-cineole satisfies the rule of Ghose, and camphor satisfies the Muegge rule. It is worth noting that the Topological polar surface area (TPSA) is a physiochemical descriptor of polarity, which should be between 20 and 130(Å^2) and is often used to predict cellular absorption (Daina et al., 2017). Results (in Table 11) show that just the linalool has a good value of TPSA (20.23Å^2). Concerning the boiled egg (Fig, 5), on the plot, except for 1-dodecane (located in the grey area), 1,8-cineole, cis-thujone, camphor, and linalool were in the yolk, which means that the compounds had a higher chance to permeate to the brain and the 1-dodecane had a lower gastrointestinal absorption (HIA) and limited BBB penetration. Furthermore, no molecules were predicted as substrates of permeability glycoprotein (P-gp) (PGP-), then

Table 12
Toxicity prediction using ProToxII software.

Ligand	LD50 mg/kg	Toxicity Class
1,8-Cineole	2480	5
Camphor	775	4
Cis-Thujone	500	4
1-Dodecene	5050	6
Linalool	2200	5

not actively effluxed by P-gp from the central nervous system or the gastrointestinal lumen.

Concerning toxicity prediction results (LD50 and toxicity class), it showed that none of the five compounds demonstrated acute toxicity (considering class 1 as a toxic class and class 6 as a non-toxic class) with LD50 values ranging from 5oomg/kg of cis-thujone to 5050 mg/kg of 1-dodecane (Table12).

5. Conclusion

The present study reflects that rosemary, sage, and lavender essential oils had a significant antibacterial effect against *P. aeruginosa* and *K. pneumoniae* and showed a synergistic effect when combining EOs with ineffective antibiotics. This activity may be attributed to the richness of bioactive compounds. Employing molecular docking, elucidating physiochemical properties, and the ADMET-drug-likeness, we have shown that the major components of the three Essential oils 1,8-Cineole, Camphor, cis-Thyjone, 1-Dodecene, and Linalool have the potential to target and bind essential proteins for bacterial survival and have more specifcity toward the quorum sensing LasR binding domain. They could be compounds with a potent antimicrobial activit and may serve as a lead molecule. Further work is recommended to validate these findings and to develop new agents with therapeutic activity.

Declaration of competing interest

The authors declare that they have no known competing financial interests or personal relationships that could have appeared to influence the work reported in this paper.

References

Adams, R.P., 2007. Identification of Essential Oil Components By Gas Chromatography /mass spectroscopy, 4th Edition Allured Publ., Carol stream, IL.

Alaoui Jamali, C., Kasrati, A., Fadli, M., Hassani, L., Leach, D., Abbad, A., 2017. Synergistic Effects of Three Moroccan thyme Essential Oils With Antibiotic Cefixime. Phytothérapie.

Aliye, M., Dekebo, A., Tesso, H., Abdo, T., Eswaramoorthy, R., Melaku, Y., 2021. Molecular docking analysis and evaluation of the antibacterial and antioxidant activities of the constituents of Ocimum cufodontii. Sci. Rep. 11 (1).

Al-Mijalli, S.H., Assaggaf, H., Qasem, A., El-Shemi, A.G., Abdallah, E.M., Mrabti, H.N., Bouyahya, A., 2022. Antioxidant, Antidiabetic, and Antibacterial Potentials and Chemical Composition of Salvia officinalis and Mentha suaveolens Grown Wild in Morocco. Adv. Pharmacol. Pharm. Sci..

Ayub, M.A., Hanif, M.A., Sarfraz, R.A., Shahid, M., 2018. Biological activity of boswellia serrata roxb. Oleo gum resin essential oil: Effects of extraction by supercritical carbon dioxide and traditional methods. International Journal of Food Properties 21 (1), 808–820.

Chbel, A., Elmakssoudi, A., Rey-Méndez, M., Barja, J.L., Soukri, A., El Khalfi, B., 2022. Analysis of the chemical compositions of six essential oils and evaluation of their antioxidant and antibacterial activities against some drug-resistant bacteria in aquaculture. Journal of HerbMed Pharmacology 11 (3), 401–408.

Chen, C., Razali, U.H.M., Saikim, F.H., Mahyudin, A., Noor, N.Q.I.M., 2021. Morus alba l. Plant: Bioactive compounds and potential as a functional food ingredient. In Foods 10 (3).

Conde-Hernández, L.A., Luna-Guevara, M.L., Luna-Guevara, J.J., Pérez-Vázquez, J., Aranda-García, R.J., 2021. Mexican sage (Salvia officinalis) extraction using factorial design and its effect on chemical and antibacterial properties. J. Chem..

Daina, A., Michielin, O., Zoete, V., 2017. SwissADME: A free web tool to evaluate pharmacokinetics, drug-likeness and medicinal chemistry friendliness of small molecules. Sci. Rep. 7.

Daina, A., Zoete, V., 2016. A BOILED-Egg To Predict Gastrointestinal Absorption and Brain Penetration of Small Molecules. ChemMedChem. 1117–1121.

El Hadri, A., Ángeles Gómez Del Río, M., Sanz, J., Coloma, A.G., Idaomar, M., Ozonas, B.R., Benedí González, J., Isabel, M., Reus, S., 2010. Cytotoxic activity of α-humulene and transcaryo-phyllene from Salvia officinalis in animal and human tumor cells. An. R. Acad. Farm 76 (3), 343–356.

Essaqui, A., Elamrani, A., Cayuela, J.A., Benaissa, M., 2007. Chemical Composition of the Essential Oil of Warionia saharae from Morocco. Journal of Essential Oil-Bearing Plants 10 (3), 241–246.

Fadli, M., Saad, A., Sayadi, S., Chevalier, J., Mezrioui, N.E., Pags, J.M., Hassani, L., 2012. Antibacterial activity of Thymus maroccanus and Thymus broussonetii essential oils against nosocomial infection - Bacteria and their synergistic potential with antibiotics. Phytomedicine 19 (5), 464–471.

Gavanji, S., Mohammadi, E., Larki, B., Bakhtari, A., 2014. Antimicrobial and cytotoxic evaluation of some herbal essential oils in comparison with common antibiotics in bioassay condition. Integr. Med. Res. 3 (3), 142–152.

Gezici, S., Sekeroglu, N., Kijjoa, A., 2017. In vitro anticancer activity and antioxidant properties of essential oils from Populus alba L. and Rosmarinus officinalis L. from South Eastern Anatolia of Turkey. Indian Journal of Pharmaceutical Education and Research 51 (3), 498–503.

Ghadri, T., Mousavi, G.S.L., Sharafi, S.M., Darvish, A.A.S., Rezaee, M.B., 2010. Antimicrobial, antioxidant, hematologic and cytotoxic properties of Lavandula angustifolia essential oil. Pathobiology Research 12 (4), 45–58.

Govaerts, R., 2003. World Checklist of Selected Plant Families Database in ACCESS: 1-216203.. The Board of Trustees of the Royal Botanic Gardens, Kew.

Hannour, K., Boughdad, A., Maataoui, A., Bouchelta, A., 2018. Chemical composition of Rosmarinus officinalis (Lamiaceae) essential oils and evaluation of their toxicity against Bruchus rufimanus (Coleoptera: Chrysomelidae: Bruchinae) in Morocco. Int. J. Trop. Insect Sci. 38 (3), 192–204.

Hossain, S., Heo, H., De Silva, B.C.J., Wimalasena, S.H.M.P., Pathirana, H.N.K.S., Heo, G.J., 2017. Antibacterial activity of essential oil from lavender (Lavandula angustifolia) against pet turtle-borne pathogenic bacteria. Lab. Anim. Res. 33 (3), 195–201.

Jankauskaitė, V., Vitkauskienė, A., Lazauskas, A., Baltrusaitis, J., Prosyčevas, I., Andrulevičius, M., 2016. Bactericidal effect of graphene oxide/Cu/Ag nanoderivatives against Escherichia coli, Pseudomonas aeruginosa, Klebsiella pneumoniae, Staphylococcus aureus and Methicillin-resistant Staphylococcus aureus. Int. J. Pharm. 511 (1), 90–97.

Khomarlou, N., Aberoomand-Azar, P., Lashgari, ardalan P., Tebyanian, H., Hakakian, A., Ranjbar, R., Ayatollahi, S.A., 2018. Essential oil composition and in vitro antibacterial activity of chenopodium album subsp. Striatum. Acta Biol. Hung. 69 (2), 144–155.

Laxminarayan, R., Duse, A., Wattal, C., Zaidi, A.K.M., Wertheim, H.F.L., Sumpradit, N., Vlieghe, E., Hara, G.L., Gould, I.M., Goossens, H., Greko, C., So, A.D., Bigdeli, M., Tomson, G., Woodhouse, W., Ombaka, E., Peralta, A.Q., Qamar, F.N., Mir, F., Cars, O., 2013. Antibiotic resistance-the need for global solutions. In The Lancet Infectious Diseases 13 (12), 1057–1098.

Lešnik, S., Furlan, V., Bren, U., 2021. Rosemary (Rosmarinus officinalis L.): extraction techniques, analytical methods and health-promoting biological effects. In Phytochemistry Reviews 20 (6), 1273–1328.

Li, L., Li, Z.W., Yin, Z.Q., Wei, Q., Jia, R.Y., Zhou, L.J., Xu, J., Song, X., Zhou, Y., Du, Y.H., Peng, L.C., Kang, S., Yu, W., 2014. Antibacterial activity of leaf essential oil and its constituents from Cinnamomum longepaniculatum. In Int J Clin Exp Med 7 (7).

Lipinski, C.A., Lombardo, F., Dominy, B.W., Feeney, P.J., 2001. Experimental and computational approaches to estimate solubility and permeability in drug discovery and development q settings. In Advanced Drug Delivery Reviews 46.

Lister, P.D., Wolter, D.J., Hanson, N.D., 2009. Antibacterial-resistant Pseudomonas aeruginosa: Clinical impact and complex regulation of chromosomally encoded resistance mechanisms. In Clinical Microbiology Reviews 22 (4), 582–610.

López, P., Sánchez, C., Batlle, R., Nerín, C., 2005. Solid- and vapor-phase antimicrobial activities of six essential oils: Susceptibility of selected foodborne bacterial and fungal strains. J. Agric. Food Chem. 53 (17), 6939–6946.

Miladi, H., Zmantar, T., Kouidhi, B., Al Qurashi, Y.M.A., Bakhrouf, A., Chaabouni, Y., Mahdouani, K., Chaieb, K., 2017. Synergistic effect of eugenol, carvacrol, thymol, p-cymene and γ-terpinene on inhibition of drug resistance and biofilm formation of oral bacteria. Microb. Pathog. 112, 156–163.

& Mohamed, W., El-Wafa, A., Rahma, Ahmed, H., Mohamed, Ramadan, A.H., 2020. x Synergistic effects of pomegranate and rosemary extracts in combination with antibiotics against antibiotic resistance and biofilm formation of Pseudomonas aeruginosa. Braz. J. Microbiol. 51 (3), 1079–1092.

Mosafa, E., Yahyaabadi, S., Doudi, M., 2013. In-Vitro Antibacterial Properties of Sage (Salvia officinalis) Ethanol Extract against Multidrug Resistant Staphylococcus aureus, Escherichia coli, Pseudomonas aeruginosa and Klebsiella pneumoniae. Zahedan Journal of Research in Medical Sciences.

Mseddi, K., Alimi, F., Noumi, E., Veettil, V.N., Deshpande, S., Adnan, M., Hamdi, A., Elkahoui, S., Alghamdi, A., Kadri, A., Patel, M., Snoussi, M., 2020. Thymus musilii Velen. as a promising source of potent bioactive compounds with its pharmacological properties: In vitro and in silico analysis. Arab. J. Chem. 13 (8), 6782–6801.

Mulyaningsih, S., Sporer, F., Zimmermann, S., Reichling, J., Wink, M., 2010. Synergistic properties of the terpenoids aromadendrene and 1,8-cineole from the essential oil of eucalyptus globulus against antibiotic-susceptible and antibiotic-resistant pathogens. Phytomedicine 17 (13), 1061–1066.

Omurtag Özgen, P.S., Biltekin, S.N., İduğ, T., Macit, C., Ayran, İ., Çelik, S.A., Kültür, Ş., Kan, Y., Omurtag, G.Z., 2022. Chemical composition and in vitro mutagenic, antioxidant and anti-inflammatory activities of Lavandula angustifolia Mill. essential oil from Turkey. Journal of Research in Pharmacy 26 (4), 781–789.

Prabuseenivasan, S., Jayakumar, M., Ignacimuthu, S., 2006. In vitro antibacterial activity of some plant essential oils. BMC. Complement. Altern. Med. 6.

Rajalakshmanan, Eswaramoorthy, Hailekiros, H., Kedir, F., Endale, M., 2021. In silico molecular docking, dft analysis and admet studies of carbazole alkaloid and coumarins from roots of clausena anisata: A potent inhibitor for quorum sensing. Advances and Applications in Bioinformatics and Chemistry 14, 13–24.

Sawant, A.A., Hegde, N.V., Straley, B.A., Donaldson, S.C., Love, B.C., Knabel, S.J., Jayarao, B.M., 2007. Antimicrobial-resistant enteric bacteria from dairy cattle. Appl. Environ. Microbiol. 73 (1), 156–163.

Shaaban, H.A., Bedair, M., Ahmed, M., El-Sideek El-Sideek, L., Amer, M.M., 2013. ORIGINAL ARTICLES Study on the antimicrobial activity and synergistic/antagonistic effect of interactions between antibiotics and some spice essential oils against

pathogenic and food-spoiler microorganisms. In Journal of Applied Sciences Research 9 (8).
Silva, V.A., Da Sousa, J.P., De Luna Freire Pessôa, H., De Freitas, A.F.R., Coutinho, H.D.M., Alves, L.B.N., Lima, E.O., 2016. Ocimum basilicum: Antibacterial activity and association study with antibiotics against bacteria of clinical importance. Pharm. Biol. 54 (5), 863–867.
Slimani, C., Sqalli, H., Rais, C., Farah, A., Lazraq, A., Ghadraoui, L.El, Belmalha, S., Echchgadda, G., 2022. Chemical composition and evaluation of biological effects of essential oil and aqueous extract of Lavandula angustifolia L. Notulae Scientia Biologicae 14 (1).
Sutherland, N.C.H., 2008. Catálogo de las plantes vasculares de Honduras. Espermatofitas: 1-1576. SERNA/Guaymuras, Tegucigalpa, Honduras
Trott, O., Olson, A.J., 2009. AutoDock Vina: Improving the speed and accuracy of docking with a new scoring function, efficient optimization, and multithreading. Journal of Computational Chemistry. NA-NA..
Van Vuuren, S.F., Suliman, S., Viljoen, A.M., 2009. The antimicrobial activity of four commercial essential oils in combination with conventional antimicrobials. Lett. Appl. Microbiol. 48 (4), 440–446.
Varela, M.F., Stephen, J., Lekshmi, M., Ojha, M., Wenzel, N., Sanford, L.M., Hernandez, A.J., Parvathi, A., Kumar, S.H., 2021. Bacterial resistance to antimicrobial agents. Antibiotics 10 (5).
Wang, W., Li, N., Luo, M., Zu, Y., Efferth, T., 2012. Antibacterial activity and anticancer activity of Rosmarinus officinalis L. essential oil compared to that of its main components. Molecules. 17 (3), 2704–2713.
World Health Organisation (WHO), 2021. Comprehensive Review of the WHO Global Action Plan on Antimicrobial Resistance, p. 2.
Yang, S.K., Yusoff, K., Thomas, W., Akseer, R., Alhosani, M.S., Abushelaibi, A., Lim, S.H.E., Lai, K.S., 2020. Lavender essential oil induces oxidative stress which modifies the bacterial membrane permeability of carbapenemase producing Klebsiella pneumoniae. Sci. Rep. 10 (1).